Surface-Induced Dissociation Mass Spectra as a Tool for Distinguishing Different Structural Forms of Gas-Phase Multimeric Protein Complexes

Royston S. Quintyn, Mowei Zhou, Jing Yan, and Vicki H. Wysocki*

Department of Chemistry and Biochemistry, The Ohio State University, 484 West 12th Avenue, Columbus, Ohio 43210, United States

S *Supporting Information*

ABSTRACT: One attractive feature of ion mobility mass spectrometry (IM-MS) lies in its ability to provide experimental collision cross section (CCS) measurements, which can be used to distinguish different conformations that a protein complex may adopt during its gas-phase unfolding. However, CCS values alone give no detailed information on subunit structure within the complex. Consequently, structural characterization typically requires molecular modeling, which can have uncertainties

without experimental support. One method of obtaining direct experimental evidence on the structures of these intermediates is utilizing gas-phase activation techniques that can effectively dissociate the complexes into substructures while preserving the native topological information. The most commonly used activation method, collision-induced dissociation (CID) with low-mass target gases, typically leads to unfolding of monomers of a protein complex. Here, we describe a method that couples IM-MS and surface-induced dissociation (SID) to dissociate the source-activated precursors of three model protein complexes: C-reactive protein (CRP), transthyretin (TTR), and concanavalin A (Con A). The results of this study confirm that CID involves the unfolding of the protein complex via several intermediates. More importantly, our experiments also indicate that retention of similar CCS between different intermediates does not guarantee retention of structure. Although CID spectra (at a given collision energy) of source-activated, mass-selected precursors do not distinguish between native-like, collapsed, and expanded forms of a protein complex, dissociation patterns and/or average charge states of monomer products in SID of each of these forms are unique.

N ative mass spectrometry (MS) has emerged as a powerful structural biological tool that provides information on dissociation constants,[1] binding stoichiometry and binding specificity of immune complexes,[2] and the identification and relative quantification of transient species during the subunit exchange of multicomponent protein complexes.[3] Tandem MS (MS/MS), which encompasses techniques where ions of a specific m/z are selected and dissociated, offers the added dimension of determining subunit connectivity in a protein complex by identification of subcomplexes generated upon dissociation.[4,5] Collision-induced dissociation (CID), which relies on ion activation via collisions of precursor ions with neutral gas atoms or molecules, is the most commonly used gas-phase dissociation method available in commercial mass spectrometers.[6] CID of protein complexes typically results in "asymmetric" dissociation, where a monomer is ejected with approximately half the available charge of the protein complex precursor to produce highly charged monomers and their complementary ($n - 1$) multimers.[7,8] Although it is well-established that the CID dissociation patterns observed are due to monomer unfolding which arises from multiple low-energy collisions between precursor ions and gas atoms or molecules, a number of aspects related to the CID unfolding mechanism are not fully understood.[6,9] These include aspects related to the

number of monomers that undergo unfolding, the early conformational changes present before monomer ejection, and whether charge migrates to unfolded monomers or unfolding induces charge migration.[6,10]

The coupling of ion mobility (IM) with MS provides the added dimension of identifying various conformations present for a specific protein,[11] and as a consequence IM-MS has been employed to interrogate protein unfolding in the gas phase with the aim of addressing some of the controversies mentioned above. One such example involves experiments conducted by Ruotolo et al. where the collisional activation of the 56 kDa transthyretin (TTR) tetrameric complex was followed by IM-MS measurements.[12] Experimental collision cross section (CCS) values obtained from IM-MS measurements were subsequently compared with those calculated for structures produced both by manually and computationally unfolding TTR monomers and docking these unfolded subunits onto the folded complex. From these analyses, it was established that gas-phase activation of TTR results in the presence of partially folded intermediate states that can have one or more unfolded

subunits.[12] In another study, Hall et al. conducted molecular dynamics (MD) simulations on entire protein complexes in vacuo over a linear temperature gradient of 300−800 K and demonstrated that collisional activation of protein complexes with large internal cavities, such as serum amyloid P component (SAP) and tryptophan RNA-binding attenuation protein (TRAP), initially led to collapse of the rings followed by unfolding of one or more monomers at higher collision energies.[10] Because charges were fixed in their initial MD simulations, charge could not migrate to surface area exposed due to unfolding. Thus, in separate simulations, half the charge on the protein complex was placed on surface-accessible basic residues of one monomer in its compact state (which unfolded over the course of the simulation) and the remaining charges distributed over surface-accessible basic sites of the remaining monomers to gain insight into CID. Subsequently, it was determined that the CCS of the unfolded monomer from these simulations showed good correlation with that of the monomer ejected in CID experiments, which allowed the authors to suggest that loss of an unfolded monomer occurs from asymmetrically charged protein complex ions.[10] In contrast, when simulations were conducted on the supercharged +30 SAP pentamer where the charges were evenly distributed over the five monomers, charge symmetric dissociation to form compact monomers and dimers was observed. The researchers proposed that this is due to the increased charge repulsion, which results in a lower energy difference between dissociation and unfolding pathways, allowing dissociation to occur without the need for prior unfolding.[10]

Alternatively, in simulations conducted by Fegan and Thachuk, five positive charges were placed on each monomer of TTR yielding a +20 tetrameric complex, and a coarse-grained simulation was subsequently utilized to move charges between the basic residues on the TTR tetramer at different temperatures.[13] It was observed that simulations conducted at elevated temperatures (600 K) resulted in one of the monomers having half the total charge. Furthermore, plots of the radius of gyration (R_g) of the four monomers as a function of simulation time illustrated that the values of R_g remained relatively constant with time, except for one, which grew with time. Altogether, these results allowed the researchers to conclude that charge movement is important for the unfolding of protein complexes.[13]

It is clear that all the studies described above required some form of MD simulations. However, the computational expense of MD simulations and the challenge of empirically optimizing the force field models that underlie these simulations limit both its length and accuracy.[14,15] Usually assumptions which are solely based on speculation and theory need to be made to simplify the calculations to allow the simulations to be performed within a reasonable amount of time. Hence, alternative techniques that can provide direct experimental information to support or refine the computational models can greatly increase the confidence in the simulations. One such example is the use of activation methods such as electron capture dissociation (ECD) and electron transfer dissociation (ETD) coupled with IM-MS or top-down ultraviolet photo-dissociation (UVPD) to determine the regions that unfold during CID-induced or acid-induced unfolding of protein complexes.[16−18] However, although activation methods such as ECD and ETD are successful in locating unfolded regions in protein complex unfolding intermediates, e.g., the flexible regions in both α and β chains of hemoglobin,[16] these electron-

based dissociation methods have not so far been shown to be effectively dissociate the subunits and provide high-order structural information such as subunit conformation and connectivity.

The Wysocki lab has developed the application of an alternative activation method for characterizing protein complex architecture, surface-induced dissociation (SID),[19] where ions undergo a single collision with a surface target often composed of a fluorinated alkanethiol self-assembled monolayer.[20] Because SID involves a high-energy, "sudden-energy" deposition process,[21] it allows for structurally informative direct dissociation pathways to outcompete the multistep monomer unfolding dissociation pathways. This often results in folded subcomplex products with minimal structure disruption, based on experimental evidence such as CCS and symmetric charge distribution among SID products.[7,22,23] Various protein complexes have been examined by SID.[21,24−26] We recently extended the SID work to a systematic study of three D_2 (dihedral symmetry) homotetramers and showed preferential cleavage of weak interfaces of protein complexes predicted from known Protein Data Bank (PDB) structures, further suggesting that disruption of native interfaces is involved in SID.[27]

Herein, we present a method that combines IM-MS and SID in a single instrument to characterize the effects of in-source collisional activation (or in-source CID) of three model protein complexes: C-reactive protein (CRP),[28] transthyretin (TTR),[29] and concanavalin A (Con A),[30] with the aim of obtaining direct experimental evidence on the structures of their collapsed and expanded/unfolded intermediates. Protein complexes used in this study were primarily chosen based on the fact that their gas-phase unfolding behavior has been studied extensively and widely reported in the literature.[12,31−33] CRP is a homopenta-meric protein complex that increases during inflammation and that collapses and unfolds upon CID, depending on the energy input. TTR is a tetrameric carrier protein that transports the thyroid hormones and retinol bound to protein and unfolds stepwise upon CID. Con A is a tetrameric lectin, a carbonhydrate binding protein, and shows limited unfolding over a wide CID energy range.

■ EXPERIMENTAL METHODS

Reagents. Protein complexes utilized in this study included C-reactive protein and serum amyloid P (EMD Chemicals Inc., San Diego, CA), avidin (Thermo Scientific Pierce Biotechnology, Rockford, IL), and transthyretin and concanavalin A (Sigma-Aldrich, St. Louis, MO). Protein samples were diluted to 10 μM and buffer-exchanged into 100 mM ammonium acetate (AA, pH = 7.0) with size exclusion chromatography spin columns (Micro Bio-Spin 6, Bio-Rad, Hercules, CA, U.S.A.). A solution of 100 mM triethylammonium acetate (TEAA) was added to the protein samples in a 1:4 (TEAA/AA) v/v ratio to produce charge-reduced protein because reduced charge proteins, with a few charges less than with AA, typically provide structural information more reflective of known crystal structures.

Instrument Modification and Operation. Nanoelectrospray ionization mass spectrometry (nano-ESI MS) analysis was conducted by utilizing a modified quadrupole ion mobility time-of-flight (Q-IM-TOF) instrument (Synapt G2, Waters Corp., Manchester, U.K.) with a customized SID device installed either before the IM cell (SID-IM experiments where the CCS of dissociation products are determined) or

after the IM cell (IM-SID experiments where the various conformations of the source-activated precursor are separated and then dissociated by SID) as previously described.[23,34] All nano-ESI MS experiments were conducted using a capillary voltage of 1.0−1.2 kV and were carried out at cone voltages of 50, 160, and 200 V (unless otherwise stated). No heating was applied to the cone. The procedures for preparation of the nano-ESI glass capillaries and collision surfaces can be found elsewhere.[35] The following instrumental conditions were used: 5 mbar for the source/backing pressure, 2 mbar for the nitrogen gas pressure in the IM cell, rate of 120 mL/min for the flow of gas into the helium cell, $\sim 6 \times 10^{-7}$ mbar in the TOF analyzer. Both CID and SID experiments were conducted at various collision energies for the cone-activated precursors. However, for the purpose of this manuscript, CID and SID spectra are shown at collision energies that best represent all dissociation pathways observed at the various collision energies sampled.

Determination of Collision Cross Section. Collision cross section calibration curves were generated as described elsewhere in literature,[36] using four protein complexes as standards: transthyretin, avidin, concanavalin A, and serum amyloid P. All voltages in the instrument were tuned to ensure that activation between optical devices was minimized without compromising the transmission of ions. The IM wave conditions chosen (wave velocity, 300 ms^{-1}, and wave height, 20 V) yielded an R^2 value of 0.998 for the calibration plot.

Crystal structures of CRP (1GNH), TTR (1F41), and Con A (3CNA) were obtained from the Protein Data Bank. Hydrogen atoms were subsequently added to the crystal structures with PyMOL and the theoretical CCS values of the native complex calculated using the projection approximation (PA) model[37] implemented in the open source software MOBCAL.[38,39] The CCS values obtained were corrected as previously described[10] because the PA model typically underestimates CCS by approximately 14%.[39] The MOBCAL calculations were performed on the High Performance Computing servers at The Ohio State University.

RESULTS AND DISCUSSION

IM-MS Characterization of In-Source CID-Induced Unfolding of the Protein Complex. A significant amount of evidence suggests that protein complexes, when activated by CID in the ion source or a gas collision cell, may deviate from their "native-like" structures to the point of partial or complete unfolding.[12,40] In this study, we first monitored the change in drift times of specific reduced-charge states of the three protein complexes (CRP, TTR, Con A) as a function of increasing cone voltages. Extra activation was minimized after the source region without compromising the transmission of ions by appropriate tuning of voltages and gas flow rates in the instrument. The drift times were then converted to CCSs, and plots of the CCS versus cone voltage were generated for the three protein complexes (Figure 1). It is evident from Figure 1 that CRP (experimental CCS, 6550 Å^2, vs calculated CCS, 6546 Å^2), TTR (experimental CCS, 3450 Å^2, vs calculated CCS, 3327 Å^2), and Con A (experimental CCS, 5443 Å^2, vs calculated CCS, 5550 Å^2) each exist in a "native-like" structure at relatively low cone voltages. Here, the term "native-like" is used to describe a precursor ion that has a CCS value similar to that calculated for its corresponding crystal structure. On further examination of Figure 1, it is also apparent that cone activation of the protein complexes studied here results in
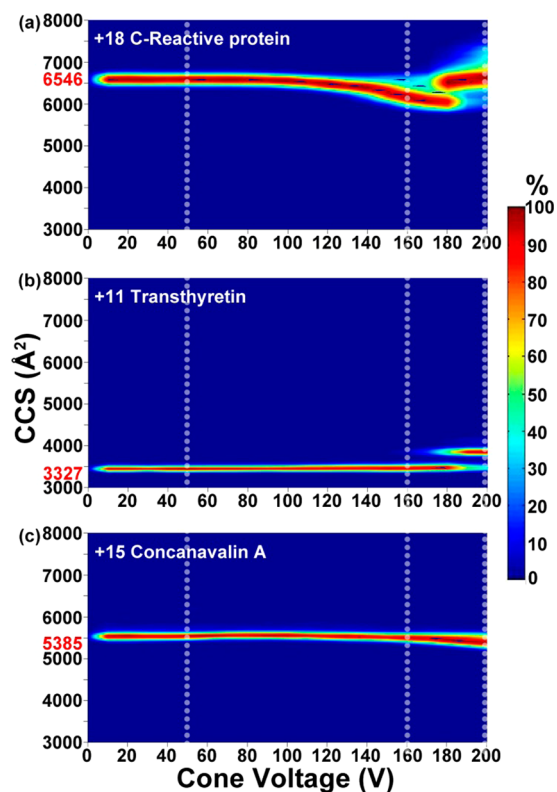

Figure 1. Effect of in-source collisional activation on the CCS of (a) +18 CRP, (b) +11 TTR, and (c) +15 Con A precursors. The theoretical CCS values calculated using the CRP crystal structure are shown in red. The cone voltages at which the protein complex precursor is chosen for further CID and SID dissociation are highlighted by the white dotted lines.

varying degrees of compaction and unfolding. Figure 1a illustrates that in addition to the "native-like" state observed at low cone voltages, CRP also exists in at least two distinct conformations—a collapsed state (6050 Å^2 at 160 V) and an expanded state (7150 Å^2 at 200 V) at elevated cone voltages. The collapse observed for CRP is expected, as it is homologous to SAP and has ringlike topology with a pore diameter of 30 Å, and has been reported previously.[31,41] In contrast, the TTR tetramer, which is a dimer of dimers with D_2 symmetry,[42] does not collapse at elevated cone voltages. Instead, at cone voltages higher than 170 V, a small subset of the TTR appears to exist in the "native-like" state, whereas the majority is present in an expanded conformation of 3850 Å^2 (Figure 1b). The in-source collisional activation of Con A appears to result only in a minor collapse (2.9%) of the Con A tetramer at the highest cone voltages accessible in our instrument (Figure 1c). Altogether, these results confirm that IM-MS is a useful initial structural tool in establishing the measurable CCS differences induced by collisional activation, but IM-MS does not characterize how and whether the structure has changed when there is no significant change in CCS. In order to directly characterize the source (or CID cell) induced conformational changes observed for these three protein complexes, even at similar CCS, further structural analysis is needed. It is not clear, for example, whether the collapsed structure simply fills the cavity with still-folded monomers or whether collapse is aided by restructuring of at least one monomer.

SID of In-Source Collisionally Activated CRP, TTR and Con A. Figure 1a can be separated into three stages based on
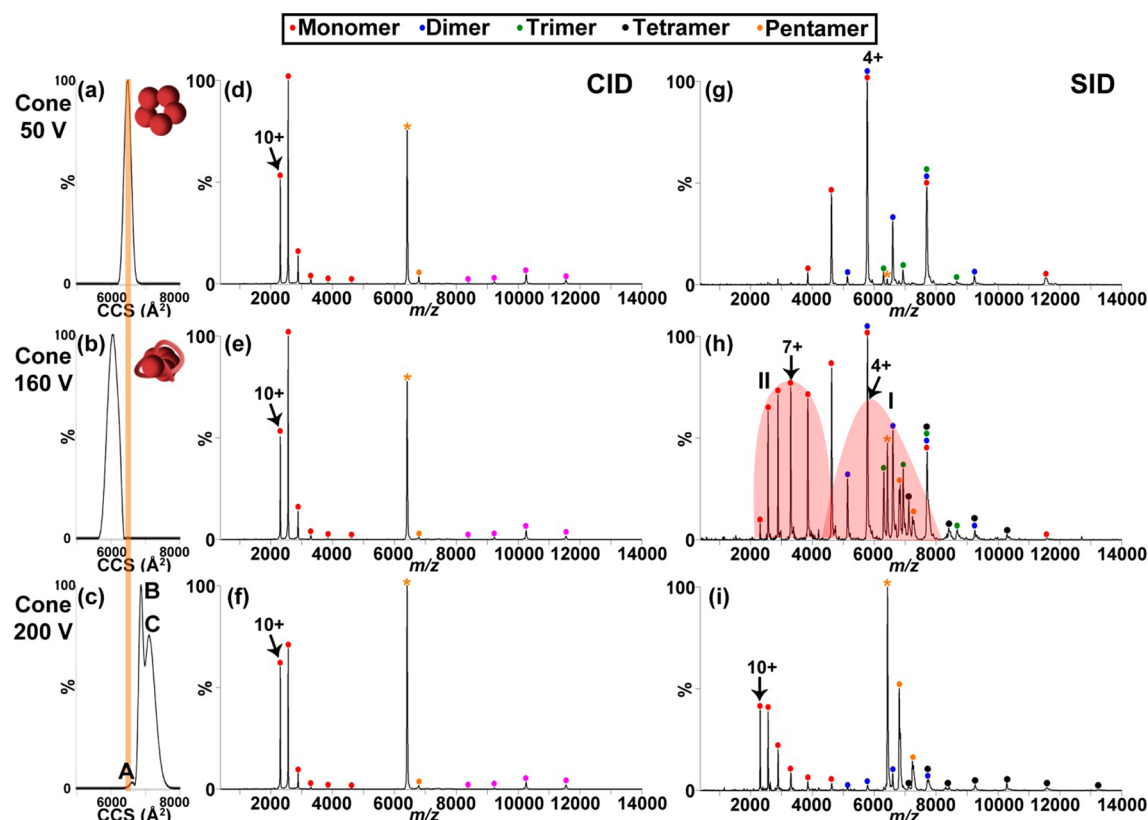
Figure 2. Effect of in-source collisional activation on the CID (2160 eV) and SID (1260 eV) dissociation products of CRP. CCS plots of the +18 CRP precursor (m/z = 6390) at cone voltages of (a) 50, (b) 160, and (c) 200 V. The theoretical CCS calculated using the CRP crystal structure is highlighted by orange vertical line, and cartoons representing the proposed structures of the various conformations present are shown in the inset. Representative CID and SID spectra are also shown at cone voltages of (d and g) 50, (e and h) 160, and (f and i) 200 V. CID yields monomer and complementary tetramer regardless of cone voltage, whereas SID yields products reflective of the native topology at cone 50 V and more CID-like products (monomer and tetramer) at cone 200 V.

the differences in CCS observed upon collisional activation of the +18 CRP pentameric complex. These three stages are in excellent agreement with the results of analyses of the radius of gyration (R_g) of the structures obtained from MD simulations conducted by Hall et al.[18] for the analogous +18 SAP pentamer. It was determined that at lower temperatures (stage I), the initial ringlike structure of SAP is retained, as little change in R_g was observed. In stage II, there was a decrease in R_g, which was associated with the symmetrical ring topology distorting into a buckled ring, whereas stage III was marked by an increase in R_g, which is consistent with the extension of one or more monomers.[10]

We have previously observed minimal unfolding of the model protein complexes in this study by surface-induced dissociation. In other words, it is expected that the dissociation patterns observed in SID provide insight into the structure of precursor ions as they exist just prior to collision with the surface.[23,43] Hence, in this study, we decided to first use IM-MS to obtain information on the global conformational changes induced by collisions with gas, and then utilize the surface-induced dissociation patterns of the conformationally altered structures as a direct measure of the conformation of each subunit. It is also sometimes possible to distinguish different protein conformations by monitoring charge state distributions of protein ions obtained from nano-ESI MS experiments, as a compact protein typically has lower charge states than the same protein in an unfolded conformation.[44,45] We hypothesize that dissociation of the various conformations observed for CRP,

TTR, and Con A by SID should yield different dissociation patterns. SID dissociation of the more unfolded conformations should produce higher charge state dissociation products. To test this hypothesis, the same precursor charge states used in the previous IM-MS experiments (Figure 1) were activated (in the source) at three selected cone voltages (50, 160, and 200 V) and subsequently dissociated via CID and SID. These cone voltages were chosen based on the differences in CCS observed in Figure 1.

C-Reactive Protein. Although it is clear from Figure 1a that a different source-produced conformation exists for CRP at each of the three cone voltages indicated by the white dotted vertical lines, downstream CID dissociation of the +18 CRP pentamer yields highly charged monomers and their complementary tetramers regardless of source cone voltage (Figure 2d−f). In contrast, the dissociation patterns observed in SID experiments of the three different source-produced conformations, produced sequentially at the three cone voltages sampled, are clearly different (Figure 2g−i). At a cone voltage of 50 V, the CCS of the intact +18 CRP pentamer is in excellent agreement with the calculated CCS obtained using the CRP crystal structure (Figure 2a, orange vertical line is calculated CCS). SID dissociation of the +18 CRP pentamer yields primary low-charged monomers with the +4 monomer being the most abundant (Figure 2g), rather than the +9 monomer dominant in CID spectra. This symmetric charge partitioning (+18 charges/5 monomers = 3.6 charges/monomer), coupled with the fact that the experimental CCS of the monomers and

dimers show good correlation with their corresponding calculated CCS values based on clipping them from crystal structure, confirms that the CRP precursor exists in a "native-like" conformation at cone 50 V (represented by the cartoon structure inset in Figure 2a). At cone 160 V, the CCS of the CRP pentamer reflects a 7.6% decrease relative to that obtained for the "native-like" conformation (Figure 2b). As mentioned earlier, this decrease in CCS has previously been attributed to the collapse of the central cavity,[10] which results in a more compact CRP pentamer. SID dissociation of the compact +18 CRP pentamer produced at cone 160 V yields two charge state distributions for the monomers (Figure 2h) with the SID dissociation pattern observed for the charge state distribution centered at +4 monomer (labeled as "I") similar to that obtained at cone 50 V. Thus, we speculate that although source activation results in collapse of the CRP pentamer, at least some of the individual monomers still retain "native-like" structure and charge consistent with the initial folded form. However, the presence of a second charge state distribution centered at the higher charged +7 monomer (labeled as "II") suggests that the collapse is not just a simple rearrangement of "folded" monomers. An examination of the experimental CCS of the higher charged monomers produced by SID-IM experiments reveals that their CCS values (ranging from 2466 to 3331 Å^2) are considerably larger than those obtained for the low-charged monomers (1960 Å^2). This suggests source unfolding of the monomer or source production of a collapsed pentamer with at least one monomer that is easier to partially unfold by SID. Thus, we propose that the conformation of CRP present at cone 160 V consists of a partially unfolded monomer, which adheres to the other four subunits (represented by the cartoon structure in Figure 2b). This is not surprising, as it has been previously reported that compact intermediates can exist in multiple structural forms: native-like regions connected by disordered regions, or a core native-like structure surrounded by unfolded or relatively unfolded polypeptide.[46,47]

An inspection of the CCS plot shown in Figure 2c reveals three conformations for the CRP pentamer at cone 200 V with conformations "B" and "C" having significantly larger CCS than the conformations seen at cone 50 and 160 V. The SID dissociation pattern observed for the +18 CRP pentamer (all three conformations) at cone 200 V (Figure 2i) is similar to that seen for CID of CRP with or without cone activation (Figure 2f), which suggests that at least one of the monomers on the CRP pentamer is unfolded. The SID dissociation products observed for pentamers activated by cone 200 V is largely due to dissociation of the more extended conformations "B" and "C", which are present at relatively higher abundances. In order to determine whether there is any difference in dissociation of conformations "A", "B", and "C" of Figure 2c we employed IM-SID. Previous work in our group has shown that the IM-SID configuration is beneficial in separating the different conformations by IM, followed by exploring these differences by SID.[48] Because SID occurs after the IM cell, the SID dissociation products that correspond to each of the three conformations can be identified by extracting spectra at drift times corresponding to an individual conformation. The results of the IM-SID experiment conducted for +18 CRP at cone 200 V are shown in Figure 3. The extracted SID spectrum observed for the very minor conformation "A" (Figure 3d) is similar to that seen for the collapsed conformation at cone 160 V (Figure 2h) where two charge state distributions are observed. Interestingly, the higher charge state distribution appears to
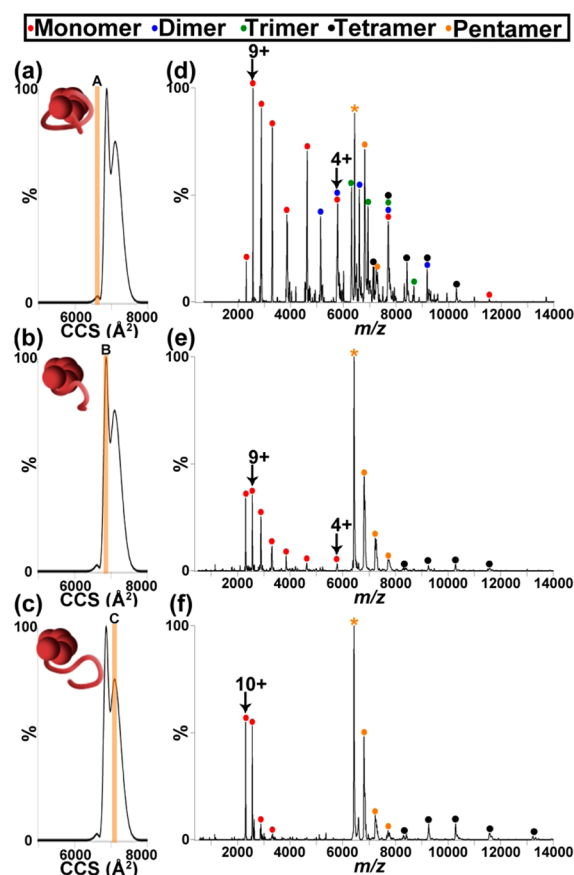

Figure 3. IM-SID of the various conformations of CRP at cone 200 V yields different SID dissociation patterns. The right panel shows the extracted SID spectra (at a collision energy of 1260 eV) of the highlighted regions in the CCS plots (left panel). Cartoons representing the proposed structures of the various conformations present are also shown in the inset of the CCS plots.

shift to even higher charge states with the most abundant peak being the +9 monomer, as compared with the +7 monomer at cone 160 V. Therefore, we propose that the conformation "A" at cone 200 V exists as a "compact" pentamer with a more unfolded monomer that adheres to the other four subunits (represented by the cartoon structure in Figure 3a). The products observed by SID of conformations "B" and "C" at cone 200 V are more "CID-like" and monomers are of higher charge, which suggests that these conformations both consist of at least one unfolded monomer. The monomers that dissociate from conformation "B" (Figure 3e) have a broad charge state distribution, with a small proportion of low charge states still present. Additionally, the percentage of lower charged monomers (+2 to +5) observed for conformation "B" (32.1%) is much less than that seen for conformation "A" (68.3%). Hence, we speculate that the unfolded monomer in conformation "B" is more extended than that in conformation "A" (represented by the cartoon in Figure 3b). The smaller percentage of low-charged monomers observed for conformation "C" in Figure 3f (4.6%) coupled with the fact that the average charge state calculated for the monomers is +9.1 (as compared with +8.1 for conformation "B"), suggests that one of the monomers in conformation "C" has more extensively unfolded during in-source collisional activation (represented by the cartoon structure in Figure 3c). The complementary tetramer products also appears to have increased in relative

intensity for conformation "C" and is likely restructured as a compact low CCS tetramer as also seen for direct CID of CRP. It is also evident that the relative abundance of undissociated precursor increases with increasing cone voltage. This phenomenon is described in the Supporting Information and further illustrated in Figure S1.

Altogether, these results not only demonstrate the capability of SID to be utilized as a means of directly probing the early conformational changes of a collisionally activated protein complex (before monomer ejection), but also indicate that these conformational changes are primarily due to the unfolding of one monomer. The fact that different unfolding intermediates produced from in-source collisional activation of CRP results in different SID dissociation patterns, whereas CID of those unfolding intermediates (which is known to result in unfolding followed by dissociation) yields similar dissociation patterns regardless of how unfolded the precursor ions are prior to CID suggests that SID does not induce additional unfolding for CRP. Hence, the differences observed in SID are due to the source-induced collision activation. Interestingly, as the cone voltage increases to activate +18 CRP pentameric precursor, the average charge state observed for the monomers increases (+4.1 at 50 V. 6550 $Å^2$, +5.8 at 160 V, 6050 $Å^2$, and +9.1 at 200 V, 7150 $Å^2$). Therefore, IM-SID also produces direct experimental evidence suggesting incremental charge migration to the unfolded monomer.

Transthyretin. CID and SID analysis was also performed on the source-activated +11 TTR precursor with CCS plots of different in-source collisionally induced conformations shown in Figure 4a−e (cone voltages 50, 160, and 200 V). In parallel with CRP, CID of the +11 TTR tetramer yields highly charged monomers (+5 and +6) and their complementary $(n - 1)$-mers (trimers in this case) regardless of cone voltage (Figure S2). Because two conformations are observed for the TTR tetramer at cone 160 V (Figure 4, parts b and c) and 200 V (Figure 4, parts d and e), we utilized IM-SID to separate and characterize the structures of the various conformations present during the gas-phase unfolding of TTR. As mentioned earlier, TTR is a dimer of dimers,[42] and thus, dissociation reflective of the native topology of TTR is expected to produce dimers.[49] However, although SID dissociation (at a collision energy of 770 eV) of the +11 TTR tetramer at cone 50 V yields primarily dimers (as highlighted by the blue vertical lines), it is clear that there is also a considerable amount of monomer and trimer present (Figure 4f). Previous studies conducted within the Wysocki lab have demonstrated that this is due to the relatively similar total interface area needed to be cleaved to produce dimer (1398 $Å^2$) versus monomer plus trimer (1573 $Å^2$) and the fact that the SID energy chosen is high enough to produce both sets of cleavage products.[27] The charge on the monomer (+4 to +6) is higher than might be expected by symmetric charge partitioning (+11/4 = +2.75/monomer), which suggests that even in SID and even when monomer is still relatively compact (see below), charge may transfer between departing subunits. The fraction of dimers produced from SID dissociation of the +11 TTR tetramer is higher at a lower SID collision energy (Figure S3), and thus confirms that TTR exists in a "native-like" conformation at cone 50 V (represented by the cartoon in Figure 4a).

It is evident from Figure 4, parts b and d, that the CCS of conformations "A" at cone 160 and 200 V have similar values to that observed for the "native-like" conformation present at cone 50 V. However, an examination of the extracted SID spectra
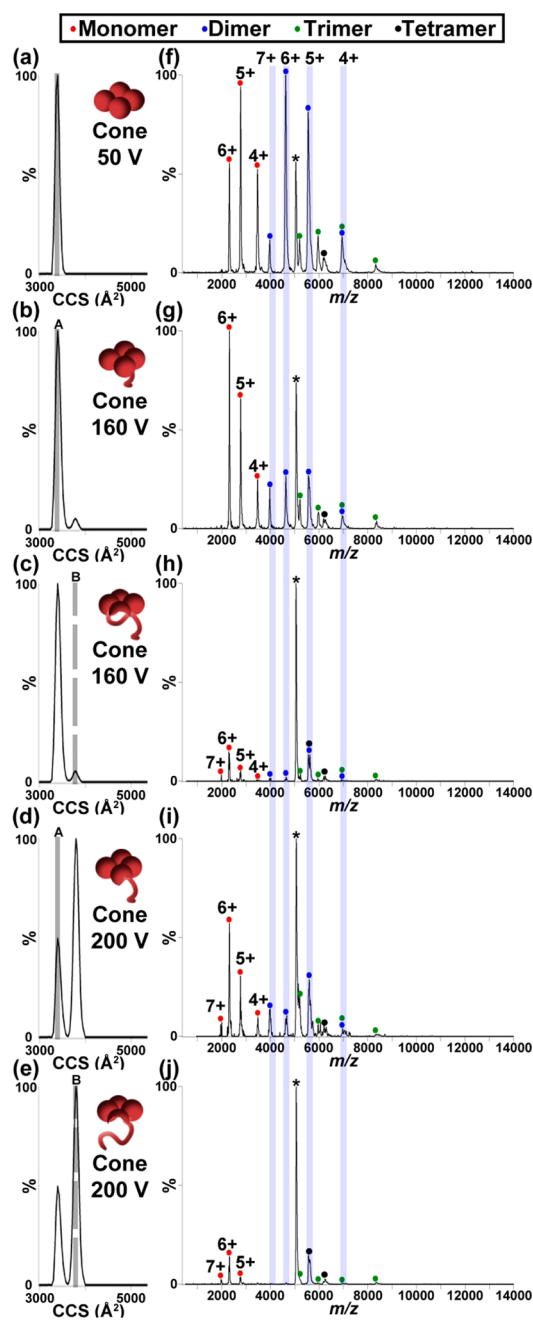

Figure 4. IM-SID of the various conformations of +11 TTR yields different SID dissociation patterns. CCS plots (left panel) and the extracted SID spectra (right panel) of the highlighted regions at a collision energy of 770 eV are shown for cone (a and f) 50, (b and g, c and h) 160, and (d and i, e and j) 200 V. Cartoons representing the proposed structures of the various conformations present are also shown in the inset of the CCS plots, while the peaks in the SID spectra corresponding to TTR dimers are highlighted in blue.

obtained from IM-SID experiments for conformations "A" at cone 160 V (Figure 4g) and 200 V (Figure 4i) illustrates differences in their dissociation patterns as compared to that observed for cone 50 V (Figure 4f). First, SID dissociation of conformations "A" present at both cone 160 and 200 V yields a lower abundance of dimers and a higher fraction of monomers. Second, the unfolded +6 monomer (1770 $Å^2$) is the most abundant monomer observed at cone 160 and 200 V, whereas the more "folded" +5 monomer (1405 $Å^2$ vs 1336 $Å^2$ for

monomer clipped from crystal structure) is the most abundant monomer at cone 50 V. Therefore, the dissociation pathway that results in cleavage of the TTR tetramer to produce monomer plus trimer for cone 160 and 200 V outcompetes the pathway that yields dimers, which suggests a structural change of tetramer. We propose that the structural change observed for these two conformations is due to local unfolding of a monomer on the TTR tetrameric complex. It was also determined that the average charge state of monomers obtained from SID dissociation of conformation "A" at cone 200 V (Figure 4i) is +5.5 (as compared with +5.3 for conformation "A" at cone 160 V and +4.9 at cone 50 V), which suggests increased charge migration as the degree of monomer unfolding increases at cone 200 versus 160 V (represented by the cartoon structures shown in Figure 4, parts b and d). Although IM-SID of conformations "B" at cone 160 and 200 V yields primarily high-charged monomers, there is also a small fraction of dimers present at cone 160 V (Figure 4h). Again, these results suggest that conformation "B" at cone 160 and 200 V may have slightly varied degrees of unfolded monomer. However, the unfolding of the monomer in conformations "B" (represented by the cartoon structures shown in Figure 4, parts c and e) appears to occur to a greater extent than it does for conformations "A" present at the same cone voltage. The results of our IM-SID experiments on the source-activated +11 TTR suggest that SID is capable of distinguishing different structures with similar CCS.

Concanavalin A. From the CCS plots shown in Figure S4a−c it is apparent that in-source collisional activation of the Con A tetramer results in the presence of a collapsed conformation at elevated cone voltages. This collapse and resistance to unfolding of the charge-reduced Con A tetramer upon collisional activation is in excellent agreement with results previously published by the Wysocki group.[31] Although the CID dissociation patterns observed for the Con A tetramer are similar over all the cone voltages sampled (Figure S4d−f), it is noted that CID dissociation does not result in ejection of an unfolded monomer but instead produces a 7.8 kDa peptide fragment and the complementary truncated tetramer (loss of 7.8 kDa). The CID behavior observed for the Con A tetramer in our experiments is very similar to that previously described in the literature.[31,50] Con A consists of four monomers, each having two large peptide fragments (A_1 and A_2 subunits) that are noncovalently associated during post-translational modification.[51,52] Thus, we speculate that CID results in unfolding and covalent fragmentation of the A_2 subunit to produce a 7.8 kDa C-terminal peptide fragment (y_{75}). SID dissociation of the +14 Con A precursor (Figure S4g−i) at all cone voltages sampled yields a mixture of low-charged "compact" monomers, dimers, and trimers, as the total interface area that must be cleaved to produce dimer (1963 $Å^2$) versus monomer plus trimer (2064 $Å^2$) are relatively similar. This suggests that the Con A tetramer exists in a "native-like" conformation even at elevated cone voltages. However, the average charge state calculated for the monomers obtained from SID dissociation of the Con A tetramer shows a slight increase with increasing cone voltage, which may be due to partial monomer unfolding facilitating charge migration. These SID dissociation patterns observed at cone 50, 160, and 200 V allow us to speculate that collisional activation of the Con A tetramer results in collapse of the "native-like" tetramer into a more compact state coupled with partial monomer unfolding (represented by the cartoons

shown in Figure S4a−c) but not enough unfolding to release the A_2 peptide.

CONCLUSIONS

In this work, we utilized IM-MS coupled with SID as a tool to characterize the structures of the intermediates resulting from in-source activation of three protein complexes. At low source CID collision energies, protein complexes undergo multiple low-energy collisions with the background gas in the source, and thus retain their "native-like" structures. However, as CID collision energy is increased (at higher cone voltages), protein complexes experience more energetic collisions with the source background gas, which results in the stepwise unfolding of monomer and the migration of charge from the more "compact" subunits to the partially unfolded monomer. This stepwise unfolding of the protein complexes results in several unfolding intermediates being formed along the unfolding pathway that occurs prior to dissociation, some with similar CCS. Unlike collision cell CID, which gives similar fragmentation spectra regardless of the unfolding intermediate, SID gives distinct fragmentation spectra of each intermediate. For example, in-source CID of CRP (which has a large internal cavity) first yields a "collapsed" unfolding intermediate where at least one monomer partially unfolds and adheres to the other "more compact" subunits, giving rise to SID spectra with two monomer charge state distributions. In contrast, the more unfolded intermediates present at higher cone voltages gives SID spectra similar to those observed for CID (where monomer unfolding occurs before monomer ejection). Altogether, this study demonstrates that IM-MS coupled with SID provides direct experimental data for understanding the unfolding intermediates of protein complexes. Future work is needed to explore whether SID can be used to distinguish structural changes in situations such as thermal exposure or aging of protein therapeutics or for characterizing misfolded proteins implicated in disease.

ASSOCIATED CONTENT

Ⓢ Supporting Information

The Supporting Information is available free of charge on the ACS Publications website at DOI: 10.1021/acs.anal-chem.5b03441.

> Additional discussion and figures illustrating the effect of cone voltage on the fraction of undissociated precursor obtained from SID, effect of source-induced collision activation on the CID dissociation products of TTR, low-energy SID of TTR, and effect of in-source collisional activation on the CID and SID dissociation products of Con A (PDF)

AUTHOR INFORMATION

Corresponding Author
*E-mail: wysocki.11@osu.edu.

Notes
The authors declare no competing financial interest.

ACKNOWLEDGMENTS

■ REFERENCES

(1) Zhang, S.; Van Pelt, C. K.; Wilson, D. B. *Anal. Chem.* **2003**, *75*, 3010.

(2) Oda, M.; Uchiyama, S.; Noda, M.; Nishi, Y.; Koga, M.; Mayanagi, K.; Robinson, C. V.; Fukui, K.; Kobayashi, Y.; Morikawa, K.; Azuma, T. *Mol. Immunol.* **2009**, *47*, 357.

(3) Sobott, F.; Benesch, J. L. P.; Vierling, E.; Robinson, C. V. *J. Biol. Chem.* **2002**, *277*, 38921−38929.

(4) Benesch, J. L. P.; Robinson, C. V. *Curr. Opin. Struct. Biol.* **2006**, *16*, 245.

(5) Sharon, M. *J. Am. Soc. Mass Spectrom.* **2010**, *21*, 487.

(6) Benesch, J. L. P. *J. Am. Soc. Mass Spectrom.* **2009**, *20*, 341.

(7) Beardsley, R. L.; Jones, C. M.; Galhena, A. S.; Wysocki, V. H. *Anal. Chem.* **2009**, *81*, 1347.

(8) Benesch, J. L. P.; Aquilina, J. A.; Ruotolo, B. T.; Sobott, F.; Robinson, C. V. *Chem. Biol.* **2006**, *13*, 597.

(9) Wanasundara, S. N.; Thachuk, M. *J. Phys. Chem. B* **2010**, *114*, 11646.

(10) Hall, Z.; Politis, A.; Bush, M. F.; Smith, L. J.; Robinson, C. V. *J. Am. Chem. Soc.* **2012**, *134*, 3429.

(11) Jurneczko, E.; Barran, P. E. *Analyst* **2011**, *136*, 20.

(12) Ruotolo, B. T.; Hyung, S.-J.; Robinson, P. M.; Giles, K.; Bateman, R. H.; Robinson, C. V. *Angew. Chem., Int. Ed.* **2007**, *46*, 8001.

(13) Fegan, S. K.; Thachuk, M. *J. Chem. Theory Comput.* **2013**, *9*, 2531.

(14) Dror, R. O.; Dirks, R. M.; Grossman, J. P.; Xu, H.; Shaw, D. E. *Annu. Rev. Biophys.* **2012**, *41*, 429.

(15) Petrenko, R.; Meller, J. *eLS*; John Wiley & Sons, Ltd.: Hoboken, NJ, 2001.

(16) Cui, W.; Zhang, H.; Blankenship, R. E.; Gross, M. L. *Protein Sci.* **2015**, *24*, 1325−1332.

(17) Lermyte, F.; Sobott, F. *Proteomics* **2015**, *15*, 2813−2822.

(18) Cammarata, M.; Lin, K.-Y.; Pruet, J.; Liu, H.-w.; Brodbelt, J. *Anal. Chem.* **2014**, *86*, 2534.

(19) Cooks, R. G.; Terwilliger, D. T.; Ast, T.; Beynon, J. H.; Keough, T. *J. Am. Chem. Soc.* **1975**, *97*, 1583.

(20) Jones, C. M.; Beardsley, R. L.; Galhena, A. S.; Dagan, S.; Cheng, G.; Wysocki, V. H. *J. Am. Chem. Soc.* **2006**, *128*, 15044.

(21) Blackwell, A. E.; Dodds, E. D.; Bandarian, V.; Wysocki, V. H. *Anal. Chem.* **2011**, *83*, 2862.

(22) Wysocki, V. H.; Joyce, K. E.; Jones, C. M.; Beardsley, R. L. *J. Am. Soc. Mass Spectrom.* **2008**, *19*, 190.

(23) Zhou, M.; Dagan, S.; Wysocki, V. H. *Angew. Chem., Int. Ed.* **2012**, *51*, 4336.

(24) Ma, X.; Zhou, M.; Wysocki, V. *J. Am. Soc. Mass Spectrom.* **2014**, *25*, 368.

(25) Zhou, M.; Jones, C. M.; Wysocki, V. H. *Anal. Chem.* **2013**, *85*, 8262.

(26) Ma, X.; Lai, L. B.; Lai, S. M.; Tanimoto, A.; Foster, M. P.; Wysocki, V. H.; Gopalan, V. *Angew. Chem., Int. Ed.* **2014**, *53*, 11483.

(27) Quintyn, R. S.; Yan, J.; Wysocki, V. H. *Chem. Biol.* **2015**, *22*, 583−592.

(28) Shrive, A. K.; Cheetham, G. M.; Holden, D.; Myles, D. A.; Turnell, W. G.; Volanakis, J. E.; Pepys, M. B.; Bloomer, A. C.; Greenhough, T. J. *Nat. Struct. Biol.* **1996**, *3*, 346.

(29) Hornberg, A.; Eneqvist, T.; Olofsson, A.; Lundgren, E.; Sauer-Eriksson, A. E. *J. Mol. Biol.* **2000**, *302*, 649.

(30) Hardman, K. D.; Ainsworth, C. F. *Biochemistry* **1972**, *11*, 4910.

(31) Zhou, M.; Dagan, S.; Wysocki, V. H. *Analyst* **2013**, *138*, 1353.

(32) Freeke, J.; Bush, M. F.; Robinson, C. V.; Ruotolo, B. T. *Chem. Phys. Lett.* **2012**, *524*, 1.

(33) Pagel, K.; Hyung, S.-J.; Ruotolo, B. T.; Robinson, C. V. *Anal. Chem.* **2010**, *82*, 5363.

(34) Zhou, M.; Huang, C.; Wysocki, V. H. *Anal. Chem.* **2012**, *84*, 6016.

(35) Galhena, A. S.; Dagan, S.; Jones, C. M.; Beardsley, R. L.; Wysocki, V. H. *Anal. Chem.* **2008**, *80*, 1425.

(36) Bush, M. F.; Hall, Z.; Giles, K.; Hoyes, J.; Robinson, C. V.; Ruotolo, B. T. *Anal. Chem.* **2010**, *82*, 9557.

(37) Mack, E. *J. Am. Chem. Soc.* **1925**, *47*, 2468.

(38) Mesleh, M. F.; Hunter, J. M.; Shvartsburg, A. A.; Schatz, G. C.; Jarrold, M. F. *J. Phys. Chem.* **1996**, *100*, 16082.

(39) Shvartsburg, A. A.; Jarrold, M. F. *Chem. Phys. Lett.* **1996**, *261*, 86.

(40) Ruotolo, B. T.; Giles, K.; Campuzano, I.; Sandercock, A. M.; Bateman, R. H.; Robinson, C. V. *Science* **2005**, *310*, 1658−1661.

(41) Volanakis, J. E. *Mol. Immunol.* **2001**, *38*, 189.

(42) Hörnberg, A.; Eneqvist, T.; Olofsson, A.; Lundgren, E.; Sauer-Eriksson, A. E. *J. Mol. Biol.* **2000**, *302*, 649.

(43) Quintyn, R.; Zhou, M.; Dagan, S.; Finke, J.; Wysocki, V. *Int. J. Ion Mobility Spectrom.* **2013**, *16*, 133.

(44) Chowdhury, S. K.; Katta, V.; Chait, B. T. *J. Am. Chem. Soc.* **1990**, *112*, 9012.

(45) Konermann, L.; Douglas, D. J. *Rapid Commun. Mass Spectrom.* **1998**, *12*, 435.

(46) Fink, A. L. *Annu. Rev. Biophys. Biomol. Struct.* **1995**, *24*, 495.

(47) Neumaier, S.; Kiefhaber, T. *J. Mol. Biol.* **2014**, *426*, 2520−2528.

(48) Zhou, M.; Wysocki, V. H. *Acc. Chem. Res.* **2014**, *47*, 1010.

(49) Foss, T. R.; Wiseman, R. L.; Kelly, J. W. *Biochemistry* **2005**, *44*, 15525.

(50) Han, L.; Ruotolo, B. T. *Int. J. Ion Mobility Spectrom.* **2013**, *16*, 41.

(51) Wang, J. L.; Cunningham, B. A.; Edelman, G. M. *Proc. Natl. Acad. Sci. U. S. A.* **1971**, *68*, 1130.

(52) Carrington, D. M.; Auffret, A.; Hanke, D. E. *Nature* **1985**, *313*, 64.